Iranian Journal of Hydrogen & Fuel Cell 1(2018) 21-33

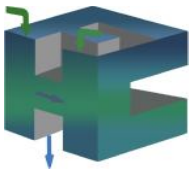

Iranian Journal of Hydrogen & Fuel Cell

IJHFC

Journal homepage://ijhfc.irost.ir

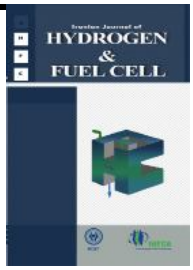

Numerical investigation of methanol crossover through the membrane in a direct methanol fuel cell

Shima Sharifi[1], Rahbar Rahimi[1,*], Davod Mohebbi-Kalhori[1], C. Ozgur Colpan[2]

[1] Department of Chemical Engineering, Faculty of Engineering, University of Sistan and Baluchestan, Zahedan, Iran.
[2] Department of Mechanical Engineering, Dokuz Eylul University, Buca, Izmir, Turkey.

Article Information

Article History:

Received:
22 Apr 2018
Received in revised form:
15 July 2018
Accepted:
21 July 2018

Keywords

Direct methanol fuel cell
DMFC
Crossover
2D model
Isothermal

Abstract

A two-dimensional, single-phase, isothermal model has been developed for a direct methanol fuel cell (DMFC). The model considers the anode and cathode electrochemical equations, continuity, momentum and species transport in the entire fuel cell. Then, the equations are coupled together and solved simultaneously using a commercial, finite element based, COMSOL Multiphysics software. The crossover of methanol is also investigated in the model. This model describes the electrochemical kinetics of methanol oxidation at the anode catalyst layer by non-Tafel kinetics. The concentration distribution of methanol, water, and oxygen was predicted by the model. In addition, the changes of methanol crossover and fuel utilization with current density were evaluated for different methanol concentrations (0.5 M, 1 M, 2 M, 4 M, and 6 M). Furthermore, it was also found that the crossover of methanol decreases at low methanol concentrations and high current densities. The results show that the polarization curve is in agreement with experimental data.

1. Introduction

The direct methanol fuel cell (DMFC) has been regarded as a promising power source for portable electronic devices and the automotive industry because of its high power density, low temperature, pressure operation, low cost, and easy fuel storage and delivery [1, 2]. DMFC includes an anode and

*Corresponding Author's Fax: 05433447092
E-mail address: rahimi@hamoon.usb.ac.ir

doi: 10.22104/ijhfc.2018.2867.1170

a cathode in which an aqueous methanol solution and oxygen are fed to the fuel and air channels, respectively. The basic oxidation, reduction, and overall electrochemical reactions for a DMFC are given in Eqs. (1-3).
At the anode:

$$CH_3OH + H_2O \rightarrow CO_2 + 6H^+ + 6e^- \quad (1)$$

At the cathode:

$$\frac{3}{2}O_2 + 6H^+ + 6e^- \rightarrow 3H_2O \quad (2)$$

Overall:

$$CH_3OH + \frac{3}{2}O_2 \rightarrow CO_2 + 2H_2O \quad (3)$$

According to the above equations the methanol is directly oxidized to bubbles and the oxygen is simultaneously reduced to water. The permeation of methanol through the membrane (methanol crossover) is a major issue which limits DMFCs cell performance; hence, many studies have focused on methanol crossover. Wang and Wang [3] presented a two-phase, multicomponent model with mixed potential effects for a liquid-feed DMFC including electrodes, channels, and PEM separator. They analyzed the transport phenomena and electrochemical kinetics and studied the effects of the methanol concentration on cell performance. Garcia et al. [4] developed a semi-analytical, one-dimensional, isothermal model of a DMFC to predict the concentration profiles in the anode and membrane as well as estimating methanol crossover. Ge and Liu [5] simulated a three-dimensional single-phase multi-component model for a liquid-fed DMFC to study various parameter effects and the effects of methanol crossover. Yan and Jen [6] presented a 2D, two-phase flow, multi-component model for the liquid-feed DMFC to evaluate the effects of various parameters such as methanol and water transport, carbon dioxide gas flow, and methanol crossover on cell performance. Colpan et al. [7] developed a two-dimensional model of a FE-DMFC to study the effects of the fluid velocity at the fuel, air, and flowing electrolyte channel inlets. Matar et al. [8] proposed a two-dimensional, single-phase, multi-component model to study the effect of changing the thickness of the cathode catalyst layer on the cell performance. The simulations considered the effects of mixed potential as well as the distribution of methanol concentration in the cathode catalyst layer, which is normally neglected in most DMFC models. Although many mathematical models are available in the literature, we have tried to present a comprehensive 2D model of a DMFC with two serpentine flow channels including all transport phenomena such as mass, species and charge transfer. The purpose of this model is to investigate methanol, water, and oxygen distribution in a fuel cell. This model also considers the crossover of methanol through the membrane from the anode to the cathode.

2. Modeling

A schematic of the DMFC used for the modeling is shown in Fig. 1. This fuel cell consists of seven layers including a fuel channel (FC), anode diffusion layer (ADL), anode catalyst layer (ACL), membrane (M), cathode catalyst layer (CCL), cathode diffusion layer (CBL) and air channel (AC). The geometrical dimensions for the 2D model are shown in Table 1.

Table 1 Geometrical Dimensions

Parameter	Value (m)
Cell length	5×10^{-2}
Anode channel thickness	1×10^{-3}
Anode GDL thickness	1.9×10^{-4}
Anode catalyst thickness	3×10^{-5}
Membrane thickness	1.75×10^{-4}
Cathode channel thickness	1×10^{-3}
Cathode GDL thickness	2.6×10^{-4}
Cathode catalyst thickness	3×10^{-5}

The following assumptions are used to simplify this model:
- Steady-state conditions.

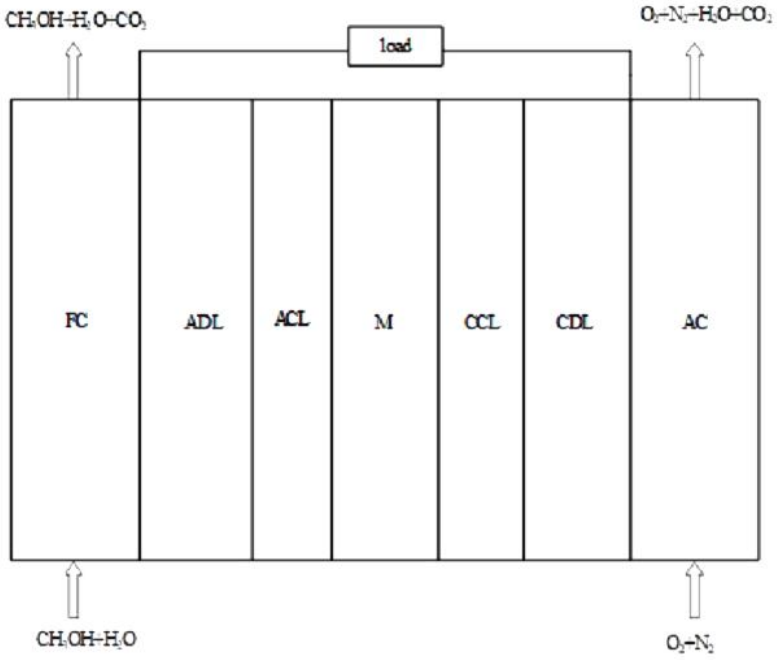

Fig. 1. 2D direct methanol fuel cell modeling geometry.

- Isothermal and incompressible operation.
- The flow is considered to be laminar.
- It is assumed that the generated remains dissolved in the solution at the anode side, so only a single phase is considered and two phase effects are not taken into account.
- The same pressure exists at the anode and the cathode.
- Methanol is fully consumed at the interface of membrane and anode catalyst layer.
- The membrane is fully hydrated.

2.2. General equations

The following conservation equations are considered for different zones: mass, momentum, species and charge transport equations. This set of equations are coupled and solved simultaneously using the available finite element based software. The following built-in modules are used in order to solve the equations:
- The Free and Porous Media Flow interface is used to solve fluid velocity and pressure distribution.
- The Transport of Diluted Species interface is used to compute the concentration fields of water, methanol, and oxygen.
- The Secondary Current Distribution interface is used to calculate the transport of charge equations.

In this study, a grid independency test was performed. A triangular mesh of 38634 elements were used to mesh the geometry. The maximum element size was set to 0.001 m. Five different segregated groups were set up to solve the set of equations and each group was solved using a direct solver, MUMPS (multifrontal massively parallel sparse).

2.2.1. Mass conservation equation

The conservation of mass is written as follows:

$$\rho \nabla .u = Q_{br} \quad (4)$$

where u is the velocity (m s^{-1}), ρ is the density (kg m^{-3}), and Q_{br} is the mass source term (k m^{-3} s^{-1}) that accounts for mass deposit and mass production in porous domains. This term is equal to zero in the flow channels and diffusion layers except in the catalyst layers due to electrochemical reactions and can be calculated by:

$$Q_{br} = \sum_m \sum_i R_{i,m} M_i \quad (5)$$

where M_i is the molecular weight of species i ($kg\,mol^{-1}$), and $R_{i,m}$ is the molar flux or source of species i for reaction m (anode or cathode) given by:

$$R_{i,m} = \frac{\nu_{i,m} i_v}{n_m F} \quad (6)$$

where i_v is the local current density of the electrochemical reaction (A m^{-3}), $V_{i,m}$ is the stoichiometric coefficient, n_m the number of participating electrons, and F is the Faraday constant (F= 96485 C mol^{-1}).

2.2.2. Momentum conservation equation

The momentum equation within the anode and cathode flow channels can be written as follows:

$$\rho(u.\nabla u) = \nabla.\left[-p + \mu(\nabla u + (\nabla u)^T)\right] + F \quad (7)$$

here, p is the pressure (Pa), μ is the dynamic viscosity (kg m^{-1} s^{-1}), and F is the body force term which accounts for the influence of volume forces such as gravity (kg m^{-2} s^{-2}).

The conservation of momentum in porous regions is defined by Brinkman equation, which includes the continuity equation, and Darcy's Law to get the velocity of fluid.

$$\frac{\rho}{\varepsilon_p}\left((u.\nabla)\frac{u}{\varepsilon_p}\right) = \nabla.\left[-p + \frac{\mu}{\varepsilon_p}(\nabla u + (\nabla u)^T) - \frac{2}{3}\frac{\mu}{\varepsilon_p}(\nabla.u)\right] - (\frac{\mu}{\kappa} + \frac{Q_{br}}{\varepsilon_p^2})u + F \quad (8)$$

where ε_p is the porosity and κ is the permeability (m^2).

2.2.3. Species conservation equation

The conservation of species is defined as:

$$N_i = -D_i \nabla c_i + u c_i \quad (9)$$

$$\nabla.(-D_i \nabla c_i) + u.\nabla c_i = R_i \quad (10)$$

where c_i is the molar concentration of the species (mol m^{-3}), D_i is the diffusion coefficient (m^2 s^{-1}), R_i is a reaction rate for the species (mol m^{-3} s^{-1}), and N_i is the molar flux (mol m^{-2} s^{-1}). Transport of chemical species by the diffusion and convection mechanisms is described in these equations.

Diffusivity is corrected in the porous media (gas diffusion layer and catalyst layer) via the Bruggeman equation as follows:

$$D_{i,eff} = \varepsilon^{1.5} D_i \quad (11)$$

in which $D_{i,eff}$ is the effective diffusivity of species i (m^2 s^{-1}).

2.2.4. Charge conservation equation

The electrochemical kinetic of the anode catalyst layer is expressed by the Meyers-Newman (non-Tafel) equation [9-11].

$$j_a = \frac{ai_{oa}^{ref} C_{MeOH} \exp((\alpha_a F / RT)\eta_a)}{C_{MeOH} + K_c \exp((\alpha_a F / RT)\eta_a)} \quad (12)$$

The Tafel equation is employed to describe the reaction of oxygen reduction on the cathode catalyst layer, namely

$$j_c + j_{xover} = ai_{oc}^{ref} \frac{C_{O_2}}{C_{O_2}^{ref}} \exp(\frac{-\alpha_c F}{RT}\eta_c) \quad (13)$$

where J_{xover} is the crossover current density, which accounts for methanol crossover flux. It can be estimated by the average molar flow rate of methanol at the interface between the membrane and cathode catalyst layer.

$$j_{xover} = \frac{6F N_{MeOH}^{"M|CCL}}{t_{ccl}} \quad (14)$$

In the above equations, α_a and α_c are the charge transfer coefficients at the anode and cathode, respectively. C_{O_2} is the oxygen concentration (mol m^{-3}), $C_{O_2}^{ref}$ is the reference oxygen concentration (mol m^{-3}), C_{MeOH} is the methanol concentration (mol m^{-3}), and ai_{oa}^{ref} and ai_{oc}^{ref} are the reference exchange current density times specific area (A m^{-3}) at the anode and

and the cathode, respectively. K_c is the rate constant of methanol oxidation (mol m^{-3}).

The overpotentials at the anode and the cathode are defined as Eqs. (15) and (16), respectively. These overpotentials are the potential difference between the solid (ϕ_s) and electrolyte phases (ϕ_l). Therefore, two charge equations, i.e., the electron and proton transport, are solved by using Ohm's law as shown in Eqs. (17) and (18).

$$\eta_a = \phi_s - \phi_l - E_a^{Eq} \quad (15)$$

$$\eta_c = \phi_s - \phi_l - E_c^{Eq} \quad (16)$$

here E^{Eq} is the thermodynamic equilibrium potential.

$$i_l = -\sigma_l \nabla\phi_l, \nabla.i_l = Q_l \quad (17)$$

$$i_s = -\sigma_s \nabla\phi_s, \nabla.i_s = Q_s \quad (18)$$

Where Q_l and Q_s are the source terms in the electrode catalyst (A m^{-3}) and σ is the electrical conductivity (S/m). Since the rate of the charge transfer reaction is described by the Butler-Volmer equation, the source terms can be written as:

For the anode side:

$$\nabla.i_l = j_a \quad (19)$$

$$\nabla.i_s = -j_a \quad (20)$$

For the cathode side:

$$\nabla.i_l = -j_c \quad (21)$$

$$\nabla.i_s = j_c \quad (22)$$

2.2.5. Boundary conditions

The boundary conditions used within the model are summarized in Table 2. For the channel inlets, flow rate and species concentrations are used. For the channel outlets, outflow and outlet pressure are used as the boundary conditions. These variables are taken as constant at some boundary conditions. For the walls, no-slip and no-flux conditions are applied.

$$u = 0 \quad (23)$$

$$-n.N_i = 0 \quad (24)$$

3. Results and discussion

3.1. Comparison with experimental data

The physical parameters used in the 2D model are presented in Table 3. To validate the 2D model, the results of the simulation are compared with experimental data [12] for a single cell as shown in Fig. 2. As can be seen in this figure, there is a good agreement with the experimental data. In order to fit the model to the experimental data, the reference exchange current density times specific area at the anode is adjusted in this paper, and are similar to those calculated by other authors [3, 4]. At high current densities, 3000 A m^{-2}, the experimental results show a deviation from linearity due to the diffusion limitations of the liquid fuel components and the limitation of reactions rates. The reason for this discrepancy at these conditions can be attributed to neglecting two-phase effects in the developed model, which has a significant effect on limiting current density.

3.2. The effects of methanol concentration

Fig. 3 shows the effects of methanol concentration on the polarization curves under the operating conditions of T= 70 , methanol flow rate of 3 ml min^{-1}, and air flow rate of 300 ml min^{-1}. It can be seen that when methanol concentration increases from 0.5 M to 4 M, the cell voltage and open circuit potential (OCV) decrease at small current densities (<1000 A m^{-2}). This is because of the methanol crossover in which some methanol molecules cannot be consumed completely in the electrochemical reaction. Some of

Table 2. Boundary Conditions used within the Model.

Variable	Symbol	Value	Units	Reference
Molar concentration				
MeOH	$C_{MeOH}^{FC,in}$	2000	mol m^{-3}	[12]
O_2	$C_{O_2}^{ac,in}$	$x_{O_2}\frac{P_{ac,in}}{RT}$	mol m^{-3}	-
H_2O	$C_{H_2O}^{in}$	$\frac{\rho_{H_2O}}{MW_{H_2O}}(1-\frac{C_{MeOH}^{in}MW_{MeOH}}{\rho_{MeOH}})$	mol m^{-3}	-
Inlet volume flow rate				
QFC	Q_{in}^{anode}	3	ml min^{-1}	[12]
QAC	$Q_{in}^{cathode}$	300	ml min^{-1}	[12]
Outlet pressures				
Anode	P_{out}^{anode}	1	atm	-
Cathode	$P_{out}^{cathode}$	1	atm	-
Electrode phase potential				
ϕ_s	$\phi_{s,FC\|ABL}$	0	V	-
ϕ_s	$\phi_{s,CBL\|AC}$	V_{cell}	V	-

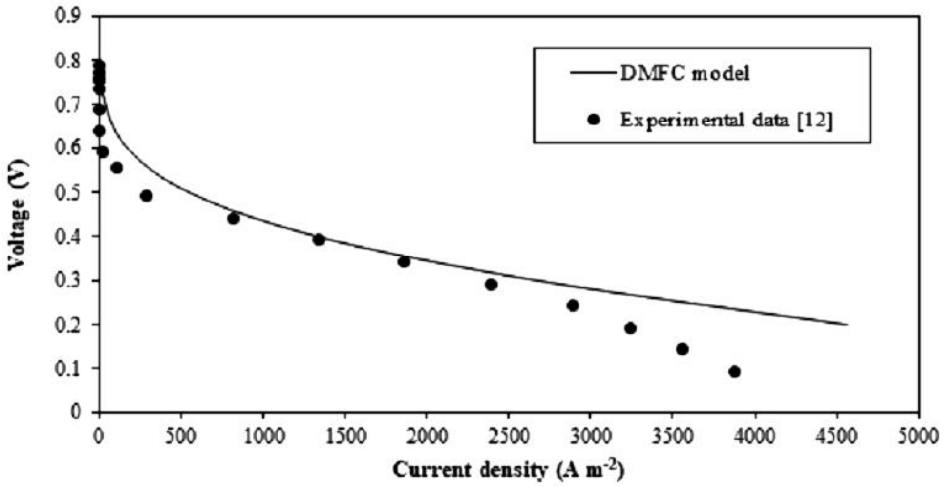

Fig. 2. Comparison of the modeling results with the experimental data.

(Methanol concentration 2M, cell temperature 70 , methanol flow rate 3 ml min^{-1}, and air flow rate 300 ml min^{-1})

the methanol penetrates through the membrane and reacts with the oxygen in the cathode.

At high current density, when the methanol concentration increases (0.5-2 M) the performance improves because the crossover is not as significant. But when the methanol concentration is more than 2 M, the cell performance decreases. This is because the crossover of methanol again affects the polarization curve.

Table 3. Physical Parameters for the 2D Model

Parameter	Value	Unit	Reference
Cell temperature	343	K	-
Pressure of the anode and cathode outlets	1	atm	-
Cell voltage	0.4	V	-
Air viscosity	2.03×10^{-5}	kg m^{-1} s^{-1}	-
Air density	1.02	kg m^{-3}	-
Viscosity of liquid	$0.458509-5.30474\times10^{-3}\mathrm{T}+2.31231\times10^{-5}\mathrm{T}^2$ $-4.49161\times10^{-8}\mathrm{T}^3+3.27681\times10^{-11}\mathrm{T}^4$	kg m^{-1} s^{-1}	[13,14]
Density of liquid	$1000-0.0178(\mathrm{T}-277.15)^{1.7}$	kg m^{-3}	[13,14]
Inlet oxygen mole fraction	0.21	-	-
Inlet methanol concentration	2000	mol m^{-3}	-
Reference oxygen concentration	0.472	mol m^{-3}	[15]
Methanol oxidation reaction constant	2.265×10^{-3}	mol m^{-3}	[10]
Porosity of diffusion layer	0.6	-	[5]
Porosity of catalyst layer	0.4	-	[5]
Porosity of membrane	0.28	-	[5]
Permeability of diffusion layer	2×10^{-12}	m^2	[6]
Permeability of catalyst layer	1×10^{-13}	m^2	-
Diffusion coefficient of methanol in water	$2.8\times10^{-9}\times e^{[2436(1/353)-(1/T)]}$	m^2 s^{-1}	[16]
Diffusion coefficient of methanol in Nafion	$4.9\times10^{-10}\times e^{[2436(1/333)-(1/T)]}$	m^2 s^{-1}	[16]
Diffusion coefficient of oxygen in air	$\left(\frac{T^{1.75}\times5.8\times10^{-8}}{27.772\times P_c}\right)$	m^2 s^{-1}	[17]
Electro-osmotic drag coefficient of water	$1.6767+0.0155\times T+8.9074\times10^{-5}\times T^2$ (T *is in* $^{\circ}C$)	-	[18]
Anodic transfer coefficient	0.5	-	[5]
Cathodic transfer coefficient	0.5	-	[5]
Membrane conductivity	10	S m^{-1}	[19]
GDL conductivity	300	S m^{-1}	[19]
Reference exchange current density times specific area at anode	8×10^{5}	A m^{-3}	Fitted
Reference exchange current density times specific area at cathode	200	A m^{-3}	[15]

3.3. Methanol crossover

Fig. 4 shows the change of methanol crossover with different methanol concentrations as a function of current density. The volumetric crossover current decreases at low methanol concentrations and high current densities. The maximum crossover is about 5.33×10^{7} (A m^{-3}) at 2.6 (A m^{-2}). For each case, methanol crossover decreases linearly with current density. Finally, the crossover current density reaches zero at the mass transport limited current.

3.4. Overall cell performance

Apart from polarization and power density curves, another key parameter used to measure DMFC efficiency is fuel utilization, defined as $FU = I/(I+I_p)\times100\%$. This parameter compares the useful current density

generated by the cell with the total current density due to methanol oxidation. The fuel utilization is significantly lower than one at high methanol concentrations as a result of the large methanol crossover-flux from the anode to cathode [20]. Figs. 5–6 illustrate power current density curves and fuel utilization as a function of current density. As can be seen from Fig. 5, when the rate of methanol consumption is low the utilization of methanol increases at low current densities. Finally, the values of utilization reached 80-90% at the limiting current density because the methanol concentration is low in the catalyst layer due to mass transport resistance. These values decrease with feeding methanol concentration. Fig. 6 shows the cell voltage and power density at T = 70 and $C^{in}_{MeOH} = 2$ M as a function of current density. As can be seen from the polarization curve, the open circuit voltage (OCV) predicted by the model is much lower than the theoretical thermodynamic equilibrium potential, 1.21 V due to the strongest methanol crossover occurring at the open circuit. The limiting current density is 3980 A/m^2 due to the mass transport resistance at the anode. Also, power density increases with increasing current density, and achieves 797 W/m^2 at a current density of 3980 A/m^2.

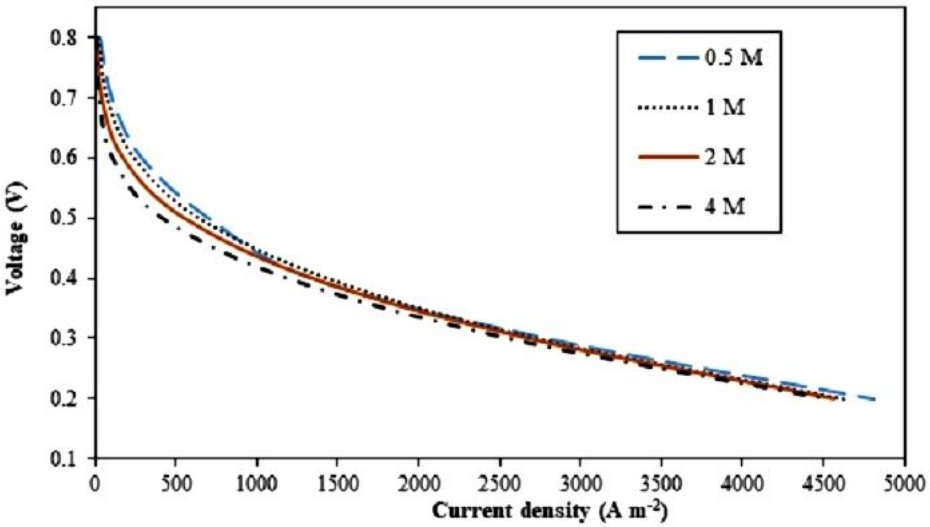

Fig. 3. Polarization curves with different methanol concentrations

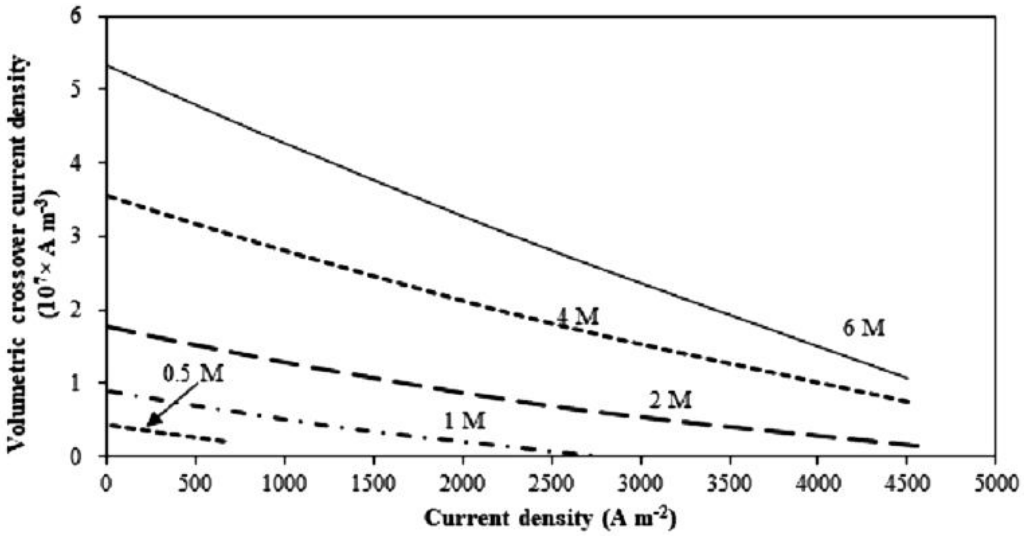

Fig. 4. Methanol crossover as a function of current density for different methanol concentrations

3.5. Species concentration distribution

The methanol concentration distribution at the cell voltage of 0.4 V is shown in Fig. 7. As shown in this figure, methanol flows through diffusion in the anode diffusion layer. The consumption of methanol at the catalyst layer leads to a decrease in methanol concentration. We assume that the methanol concentration goes to zero at the interface membrane and anode catalyst layer.

Fig. 8 shows the oxygen concentration distribution in the cathode side. The concentration decreases along the flow direction, which indicates that the oxygen is consumed at the catalyst layer due to electrochemical reaction and the oxidation of the crossover of methanol. The concentration of liquid water is presented in Fig. 9. Similar to the concentration of methanol on the anode side, the water concentration distribution decreases as a function of current density according to Eq. (1). We assumed that the membrane is fully hydrated as a result a no-flux boundary condition for the interface of the anode catalyst layer and membrane is applied.

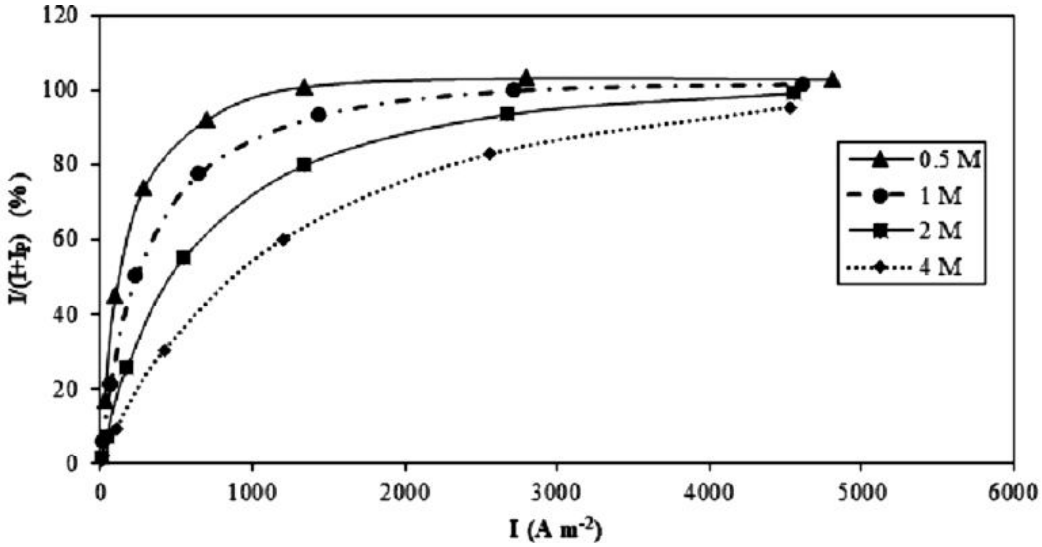

Fig. 5. Computed cell performance corresponding to T = 70 and different methanol concentrations: fuel utilization (%) as a function of cell current density

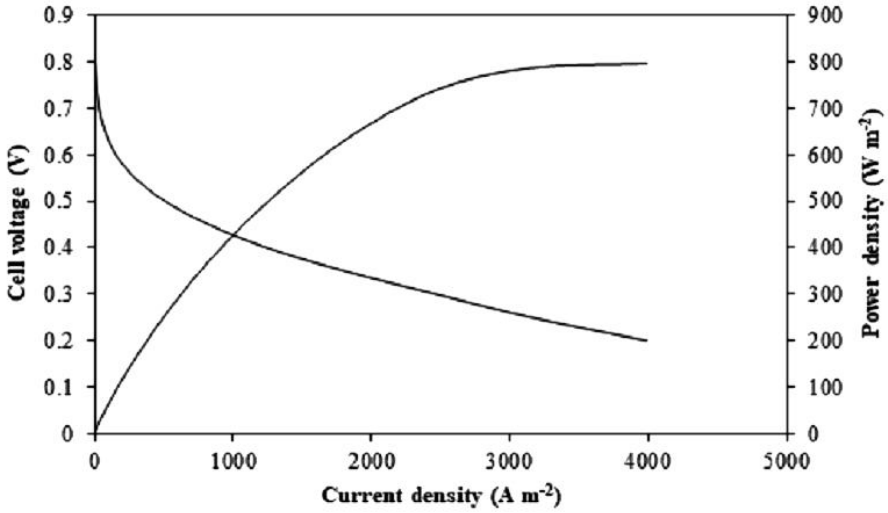

Fig. 6. Polarization curve and power density of the DMFC

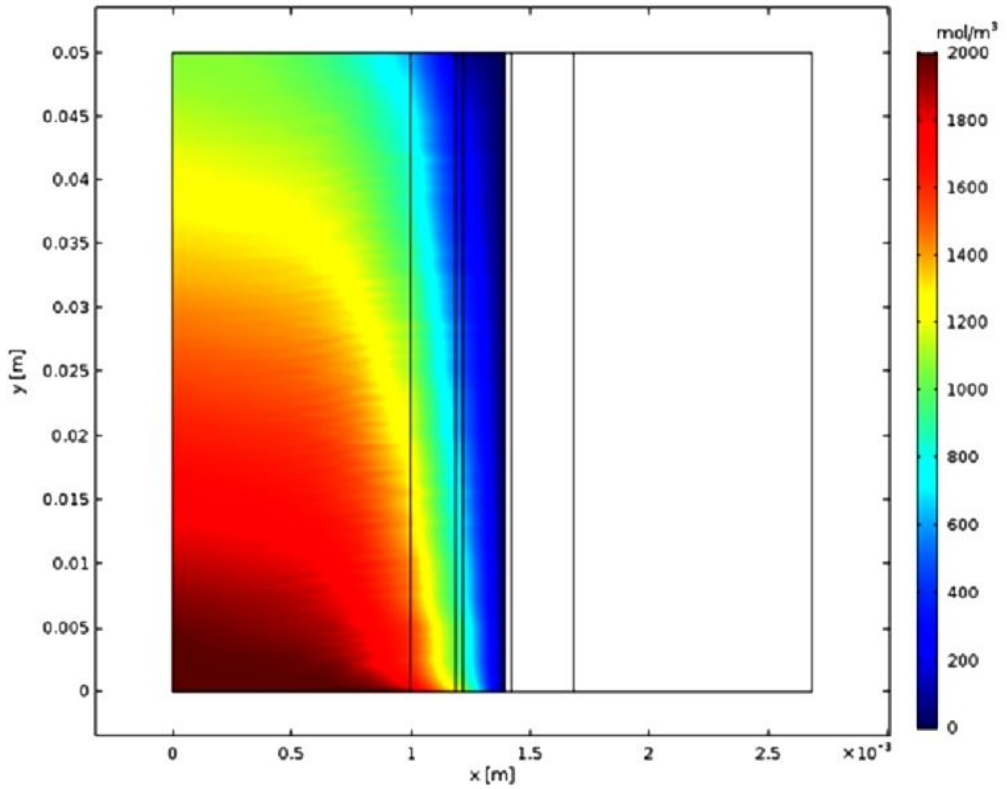

Fig. 7. Methanol concentration distribution of the DMFC

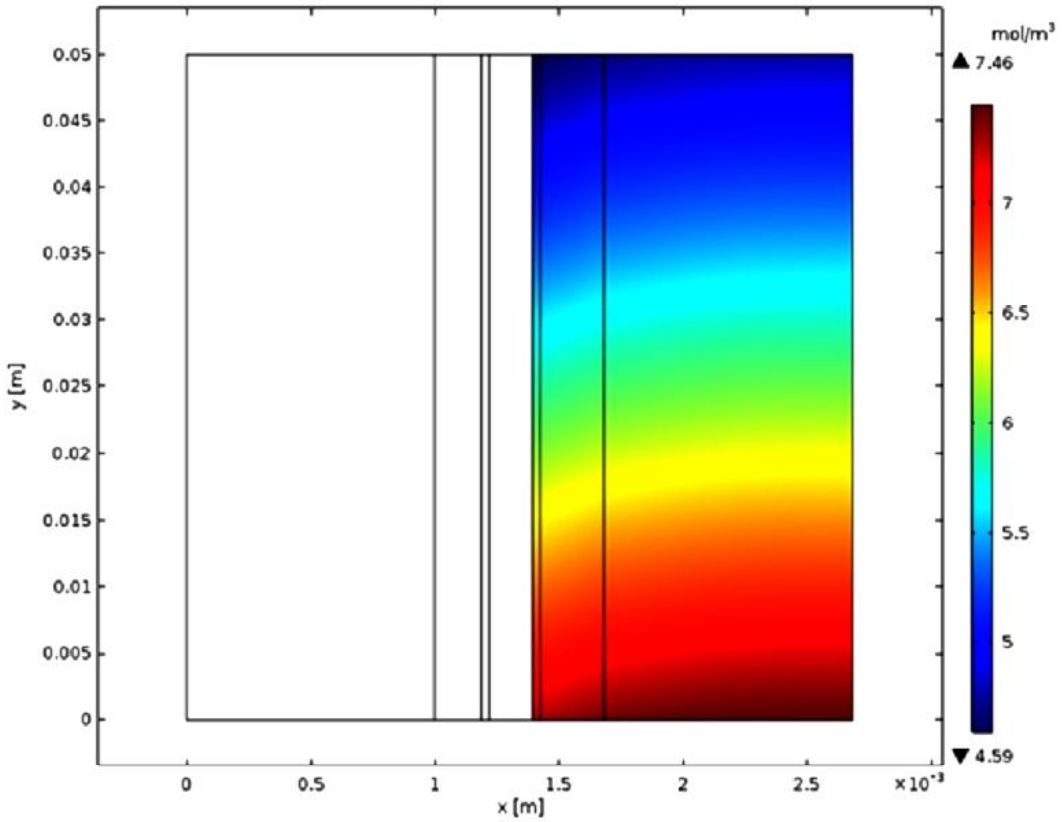

Fig. 8. Oxygen concentration distribution of the DMFC

4. Conclusions

In this work a two-dimensional, isothermal and single phase model has been developed to study the effect of the methanol crossover phenomena on the cell performance in a DMFC. The governing equations were solved using a commercially available finite element solver. In this model, the complex non-Tafel correlation of methanol electro-oxidation was applied to describe the electrochemical kinetics at the anode. The model results, including concentration distributions of species (methanol, water, and oxygen), polarization curve, power density, methanol crossover rate and fuel utilization for different methanol concentrations, were compared with experimental data and there is a good agreement between the results and the experimental data. An increase in the methanol concentration yields an increase in the methanol crossover. Moreover, the methanol concentration reduces along the flow direction due to the methanol consumption in the reaction.

Nomenclature

ai0	exchange current density times specific area (A m^{-3})
C	concentration (mol m^{-3})
D	coefficient of diffusion (m^2 s^{-1})
E^{Eq}	equilibrium voltage (V)
F	Faraday constant (s A mol^{-1})
i	current density (A m^{-2})
j	volumetric current density (A m^{-3})
j_{xover}	crossover current density (A m^{-3})
K_c	methanol oxidation reaction constant (mol m_{-3})
l	length (m)
MW	molecular weight (g mol^{-1})
n_d	electro-osmotic drag coefficient
N″	molar flow rate per cross-section (mol m^{-2} s^{-1})
P	pressure (N m^{-2})
R	universal gas constant (J K^{-1} mol^{-1})
t	thickness (m)
T	temperature of the cell (K)
u	fluid velocity (m s^{-1})
V_{cell}	cell voltage (V)
x	distance, (m); molar ratio

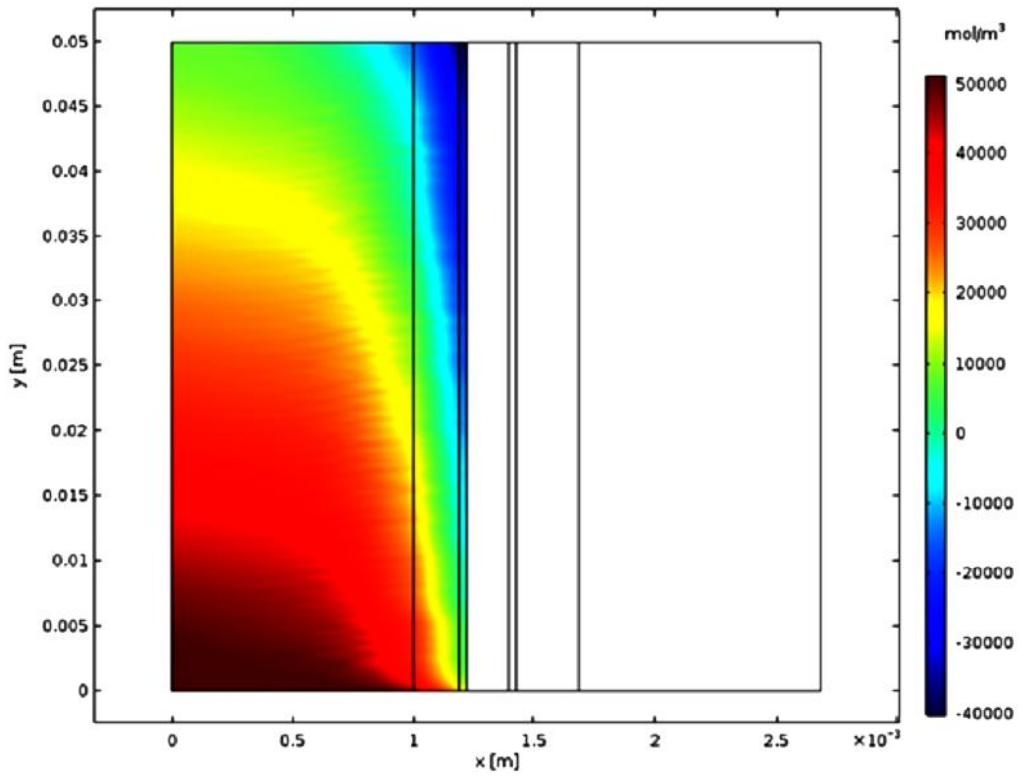

Fig. 9. Methanol concentration distribution of the DMFC

y distance (m)
w width (m)

Greek letters

α transfer coefficient
ε porosity
ρ density (g m^{-3})
σ conductivity (S m^{-1})
κ permeability (m^2)
μ dynamic viscosity (N m^{-2} s)
η overpotential (V)
p otential (V)

Subscripts/ Superscripts

a anode
c cathode
eff effective
in inlet
l electrolyte phase
MeOH methanol
s electrode phase
xover crossover
ref reference
H_2O Water
ac air channel
O_2 oxygen

References

[1] Ismail A., Kamarudin S.K., Daud W.R.W., Masdar S. and Yosfiah M.R., "Review: Mass and heat transport in direct methanol fuel cells", J. Power Sources, 2011, 196: 9847.

[2] Oliveira V.B., Rangel C.M. and Pinto A.M.F.R., "Water management in direct methanol fuel cells", Int. J. Hydrogen Energy, 2009, 34: 8245.

[3] Wang Z.H. and Wang C.Y., "Mathematical Modeling of Liquid-Feed Direct Methanol Fuel Cells", J. Electrochemical Society, 2003, 150: A508.

[4] Garcia B.L., Sethuraman V.A., Weidner J.W., White R.E. and Dougal R., "Mathematical Model of a Direct Methanol Fuel Cell", J. Electrochemical Energy Conversion and Storage, 2004, 1: 43.

[5] Ge J. and Liu H., "A three-dimensional two-phase flow model for a liquid-fed direct methanol fuel cell", J. Power Sources, 2007, 163: 907.

[6] Yang W.W. and Zhao T.S., "A two-dimensional, two-phase mass transport model for liquid-feed DMFCs", Electrochimica Acta, 2007, 52: 6125.

[7] Colpan CO., Fung A. and Hamdullahpur F., "2D modeling of a flowing-electrolyte direct methanol fuel cell", J. Power Sources, 2012, 209: 301.

[8] Matar S., Ge J. and Liu H., "Modeling the cathode catalyst layer of a Direct Methanol Fuel Cell", J. Power Sources, 2013, 243: 195.

[9] Meyers J.P. and Newman J., "Simulation of the Direct Methanol Fuel Cell - I. Thermodynamic Framework for a Multicomponent Membrane", J. Electrochemical Society, 2002, 149: A710.

[10] Meyers J.P. and Newman J., "Simulation of the direct methanol fuel cell - II. Modeling and data analysis of transport and kinetic Phenomena", J. Electrochemical Society, 2002, 149: A718.

[11] Meyers J.P. and Newman J., "Simulation of the Direct Methanol Fuel Cell - III. Design and Optimization", J. Electrochemical Society, 2002, 149: A729.

[12] Ge J. and Liu H., "Experimental studies of a direct methanol fuel cell", J. Power Sources, 2005, 142: 56.

[13] White F.M., 5th ed., Fluid Mechanics, McGraw-Hill, New York, 2003.

[14] Incropera F.D., Fundamentals of Heat and Mass

Transfer, John Wiley & Sons, New York, 1995.

[15] Shukla A.K., Jackson C.L., Scott K. and Murgia G., "A solid-polymer electrolyte direct methanol fuel cell with a mixed reactant and air anode", J. Power Sources, 2002, 111: 43.

[16] Scott K., Taama W. and Cruickshank J., "Performance and modeling of a direct methanol solid polymer electrolyte fuel cell", J. Power Sources, 1997, 65: 159.

[17] Reid R.C., Prausnitz J.M. and Sherwood T.K., "The properties of gases and liquids", McGraw-Hill, New York, 1977.

[18] Ren X. and Gottesfeld S., "Electro-osmotic drag of water in poly (perfluorosulfonic acid) membranes", J. Electrochemical Society, 2001, 148, A87.

[19] Liu W. and Wang C.Y., "Electron transport in direct methanol fuel cells", J. Power Sources, 2007, 164: 561.

[20] Vera M., "A single-phase model for liquid-feed DMFCs with non-Tafel kinetics", J. Power Sources, 2007, 171: 763.